Available online at www.sciencedirect.com
SCIENCE DIRECT®
Ecological Modelling 185 (2005) 309–327
ECOLOGICAL MODELLING
www.elsevier.com/locate/ecolmodel

Modelling buoyancy regulation in fishes with swimbladders: bioenergetics and behaviour

Espen Strand [a, *], Christian Jørgensen [a], Geir Huse [b]

[a] *University of Bergen, Department of Biology, P.O. Box 7800, N-5020 Bergen, Norway*
[b] *Institute of Marine Research, P.O. Box 1870, Nordnes, N-5817 Bergen, Norway*

Received 18 June 2004; received in revised form 13 December 2004; accepted 17 December 2004

Abstract

We present a bioenergetic model for buoyancy regulation that incorporates the restrictions and costs of swimbladder regulation with four means of hydrodynamic lift production: hovering, swimming with extended pectoral fins, swimming with adjusted tilt angle, and body lift. Previous models addressing vertical migration in fish with swimbladders have either assumed no energetic cost or a static cost of vertical migration. In this model, parameterised for Atlantic cod *Gadus morhua*, existing theory and experimental data on bioenergetics, physiology, and hydromechanics are integrated. Trade-offs and limitations were investigated from a behavioural perspective. Regulation of swimbladder volume is energetically cheap but slow. Because of the asymmetry in absorption and secretion rates with depth, fish that perform vertical migrations regularly will often be negatively buoyant and will therefore experience additional energy costs associated with hydrodynamic lift production. Hovering was optimal for slightly negatively buoyant fish, whereas tilted compensatory swimming was optimal in all other situations. The predicted optimal tilt angle was approximately 7°, and increased for small fish and for fish that were close to neutrally buoyant. The energetic saving from tilting was small for cod, and potential conflicts with other behaviours may determine when tilting would be preferential in nature. Swimbladder volumes and the corresponding energetic costs were calculated for constructed vertical migration patterns and on a set of depth data from a free-living cod. For the free-living cod, the model predicted that the fish would be neutrally or negatively buoyant, with the swimbladder being up to 40% smaller than the optimal volume.

Keywords: Atlantic cod (*Gadus morhua*); Bioenergetics model; Buoyancy regulation; Physoclist swimbladder; Tilt angle; Vertical migration; Target strength

1. Introduction

Living tissue is, with the exception of lipids, heavier than water. Aquatic organisms that intend to utilise the free water masses will therefore have to adopt some mechanism by which to control buoyancy. Nature

* Corresponding author. Tel.: +47 55 58 44 38; fax: +47 55 58 44 50.
E-mail address: Espen.Strand@bio.uib.no (E. Strand).

0304-3800/$ – see front matter © 2005 Elsevier B.V. All rights reserved.
doi:10.1016/j.ecolmodel.2004.12.013

displays a variety of solutions to this problem, ranging from constant activity via large deposits of lipids and oils, to elaborate gas-filled structures (Jobling, 1995; Schmidt-Nielsen, 1997). The degree to which some of these adaptations require energy or restrict the behavioural repertoire outlines the magnitude of the selection pressures that have shaped them (Harden Jones, 1951, 1952; Alexander, 1971, 1990, 2003; Schmidt-Nielsen, 1997).

The swimbladder found widely among teleost fishes is one solution to the buoyancy challenge. Blood-borne gases are secreted into a gas-filled cavity through a reaction that requires energy, but maintenance is energetically cheap once the gases are inside (e.g. Scholander, 1956; Prosser, 1973; Harden Jones and Scholes, 1985). The physical properties of gases, however, pose some problems. First, vertical movements make the contained gases change volume. This means that the amount of gases inside the swimbladder has to be adjusted to maintain neutral buoyancy after a change of depth. Second, gases have to be kept from escaping the swimbladder despite a pressure gradient that is proportional to depth and therefore steep at great depths (Lapennas and Schmidt-Nielsen, 1977; Ross, 1979). Third, the fish will need an organ capable of filling the swimbladder with gas against the pressure gradient found between the gasses dissolved in blood and the gasses inside the swimbladder. Gases dissolved in seawater are at best in equilibrium with sea surface conditions. The swimbladder is thus like a pressure balloon, where filling will be slower and reabsorption of gases faster at greater depths. These two conditions have implications for the vertical behaviour of the individual.

Because swimbladder adjustments take time, fish that move vertically will often be at a depth where the swimbladder volume is too large or too small to give the fish neutral buoyancy. If the fish cannot lie at the sea floor, it has to generate lift, up or down, by hydrodynamic means. Bottom-dwelling fish can often be seen hovering, waving their pectoral fins to create a downward current (Blake, 1979; Alexander, 2003). Fish that move forward through the water can use their pectoral fins as hydrofoils ('wings'), and in addition create lift with the caudal fin, by other body features, or by tilting. Hydrodynamic lift can be generated fast and can be altered quickly, but generally requires more energy than a swimbladder (Alexander, 1990, 2003).

Buoyancy regulation has hitherto not been mechanistically quantified in behavioural models studying the trade-offs involved in vertical migration. Earlier models have either assumed the cost of vertical migrations proportional to depth change (e.g. Rosland and Giske, 1994; Strand et al., 2002), assumed no cost (e.g. Clark and Levy, 1988), and have furthermore not identified the constraints imposed by a swimbladder. To improve the ecological realism of such models, this work pieces together knowledge from three research areas: swimbladder physiology, hydrodynamics of lift, and bioenergetics.

Comparisons between species have sketched the broad perspective of advantages and disadvantages with the different means of buoyancy regulation. Changes in swimbladder volume are constrained by time and depth, and hydrodynamic lift by the energy requirements. The model presented here describes the processes involved in buoyancy control: swimbladder volume changes, hovering, swimming with fins as hydrofoils and with a tilt angle. These different modes of buoyancy regulation have different rates, different energetic costs, and different constraints, and have been well-studied separately (Alexander, 1971; Blake, 1979; Harden Jones and Scholes, 1985; Vogel, 1994). By formulating them in a common bioenergetics framework, the trade-offs between the swimbladder and hydrodynamic forces as means of buoyancy regulation can be compared. The model can answer two lines of questions: (1) on the shorter time-scale, which types of behaviour are possible with regard to the physiological constraints involved, and (2) in the longer run, what are the energetic costs of the different modes of buoyancy regulation. Insights from this last approach can be used to interpret field data from free-ranging fish, and the bioenergetics currency allows comparisons of costs and benefits of different foraging behaviours to be studied. By implementing the model presented here as a submodel in behavioural models, questions into the adaptive nature of foraging behaviour and other types of behaviour involving vertical migrations in pelagic fish can be investigated.

Fish have adapted to a great range of environments, and the constraints that a swimbladder forces upon the general physoclist fish will be hard to examine. To better investigate the model's properties, species-specific values for Atlantic cod (*Gadus morhua*) were used. This is the physoclist species that has been most

extensively investigated with regard to swimbladder function (e.g. Tytler and Blaxter, 1973; Harden Jones and Scholes, 1985; Arnold and Greer Walker, 1992). Cod are known to perform vertical migrations (e.g. Brunel, 1965; Beamish, 1966; Metcalfe and Arnold, 1997; Godø and Michalsen, 2000), but the energetic cost of this behaviour with regard to variations in buoyancy has been poorly investigated. The model was applied to a time series of vertical positions recorded for cod by data storage tags (Godø and Michalsen, 2000) in order to illustrate the dynamics of the presented model's predictions.

2. Model description

The equations that describe buoyancy control in this model are intended for recalculation over several time-steps. For every time-step, the following procedure takes place: (1) the fish' depth is used as input; (2) leakage from the swimbladder is calculated based on this depth; (3) the buoyancy experienced by the fish at the actual depth is estimated based on the new state of its swimbladder (change of depth and leakage); (4) maximum rates for secretion and absorption of gases are calculated. The required secretion/absorption takes place within these limits; (5) the buoyancy not accounted for by changes in swimbladder volume has to be generated by hydrodynamic forces, i.e. through increased swimming at the optimal tilt angle, or by hovering; (6) the metabolic costs of secretion and compensatory swimming are summarised.

2.1. The swimbladder

Physoclist fish have the ability to secrete gas through a gas gland on the swimbladder wall (Prosser, 1973). The gas gland produces lactic acid and CO_2, which lower the pH and increase the concentration of solutes in the blood. Direct and indirect effects effectuate the release of haemoglobin-bound oxygen and physically dissolved gases through the Bohr, Root, and salting-out effects (Jobling, 1995; Schmidt-Nielsen, 1997; Pelster, 2001). In addition, the arterial blood supply flows through a counter-current vascular arrangement (*rete mirabile*) that multiplies blood gas tensions and maintains pH and solute concentrations in the gas gland. As a result, gas tension in the gas gland may exceed that of arterial blood several-fold, and gases thus diffuse into the pressurised swimbladder (Scholander and van Dam, 1954; Kuhn et al., 1963; Steen, 1963a). During ascents, physoclist fish will reabsorb the excess gas inside the swimbladder through a particularly vascularised area called the *oval* (Fänge, 1953; Steen, 1963b). The rate of absorption is limited, however, and rapid ascents can thus be dangerous to physoclist fish, as the swimbladder may expand beyond control or burst (Harden Jones, 1952; Tytler and Blaxter, 1973).

In this model, leakage and the maximum sustainable rates of secretion and absorption are based on gas composition with emphasis on oxygen, while the energetic cost of secretion is calculated based on physical work and a biological efficiency factor. Wherever physically dissolved gases are involved, all gases in the swimbladder are assumed to have the same physical properties as oxygen. This approximation can be partly justified since the next two components, CO_2 and N_2, have a higher and lower solubility, respectively. Furthermore, other gases (Ar, Ne, He) can be found in the swimbladder to varying degrees, and the gas composition will hence change in a complex manner resulting from past vertical behaviour. The equations relating to haemoglobin-bound oxygen use a partial pressure of oxygen in the swimbladder that is a constant fraction of the hydrostatic pressure. Because CO_2 has a higher solubility than O_2, this will tend to underestimate absorption rates during the initiation of absorption (when CO_2 would have been removed faster), but will slightly overestimate rates after the majority of CO_2 has been removed (which means that N_2 would have been more important for the overall rate of absorption) (Steen, 1963b and references therein). The model can be elaborated to incorporate gases with different physical properties, but at this point such a level of detail was not found worthwhile. The partial pressure of oxygen and other gases would then become dynamic, and the model could thus also shed light on how behavioural decisions influence the actual gas composition of the swimbladder. Although a full modelling of all gas components may be possible, it is beyond the scope of this paper.

SI units have been preferred throughout this paper, although it may seem awkward to measure the volume of the swimbladder of a small cod in cubic metres. This makes the equations easier to read, and will thus hopefully enhance understanding of the concepts involved. See Table 1 for details on all variables.

Table 1
Variables and parameters used in the model for buoyancy regulation

	Description	Value	Unit
Variables			
φ	Tilt angle	–	Degrees
Ω	Energy conversion efficiency during swimming	0.05–0.20	–
Abs_{max}	Maximum rate of O_2 absorption	–	$mol\,s^{-1}$
Act	Increase in energy expenditure during swimming	–	–
B	Buoyancy force	–	N
BL	Body length	–	m
C_{out}	Cardiac output	–	$m^3\,s^{-1}$
E_{sec}	Energy used for gas secretion	–	$J\,s^{-1}$
F_L	Pectoral fin length (at right angle from body)	–	m
L; D	Lift and drag force, subscript referring to fin, body and tilt angle (φ)	–	N
Leakage	Oxygen leakage from swimbladder	–	$mol\,s^{-1}$
M	Body mass	–	kg
MR_{HOVER}	Metabolic cost of hovering	–	$J\,s^{-1}$
MR_{PECT}	Additional metabolic cost of extended fins	–	$J\,s^{-1}$
Sec_{max}; Sec	Maximum O_2 that can be secreted into swimbladder; actual O_2 secreted	–	$mol\,s^{-1}$
SMR; TMR; AMR	Standard metabolic rate; total metabolic rate including fin drag; active metabolic rate (measured metabolism-SMR)	–	$J\,s^{-1}$
P	Hydrostatic pressure	$1 + (z/10)$	atm
S_s	Swimbladder surface area	–	m^2
Thrust	Power produced during swimming		N
U; U_H	Fish swimming speed; horizontal component	–	$m\,s^{-1}$
U_{max}	Maximum sustainable swimming speed	–	$BL\,s^{-1}$
V_n; V_s	Neutral swimbladder volume; current swimbladder volume	–	m^3
z; z_c	Depth; critical depth	–	m
Parameters			
α; β	Intercept and slope for allometric function for SMR	0.397; 0.828	–
γ	Fin beat angle during hovering	π	Radians
δ_{O_2}	Fraction oxygen in secreted gases	0.63	–
ρ_f; ρ_w	Fish tissue density; water density	1081; 1026	$kg\,m^{-3}$
ΔHb	Fraction of haemoglobin available for O_2 binding (in oval)	0.15	–
a/b	Length to width ratio of swimbladder	10	–
C_{rete}; C_{oval}	Fraction of cardiac output to *rete*; to oval	0.10; 0.25	–
E_{eff}	Energy conversion efficiency during secretion	0.10	–
$F(T)$	Temperature function for SMR	0.502 at 5 °C	–
G	Oxygen conductance	1.5×10^{-9}	$m^3\,O_2\,m^{-2}\,atm^{-1}\,s^{-1}$
g	Gravitation constant	9.81	$m\,s^{-2}$
H_{GROUND}	Energy saving during hovering due to ground effect	≤ 1	–
$[L/D]_{body}$	The lift-to-drag coefficient for body	0.75	–
O_{2a}	O_2 content of arterial blood by volume	0.10	–
O_{2sol}	Solubility of O_2	0.04	$m^3\,O_2\,m^3\,blood^{-1}\,atm^{-1}$
P_0	Pressure at surface	1	atm
R	Universal gas constant	8.206×10^{-5}	$m^3\,atm\,mol^{-1}\,K^{-1}$
		8.3144	$J\,mol^{-1}\,K^{-1}$
R_{eff}	Rete efficiency	0.20	–
T	Ambient temperature	278.15	K

Species-specific values refer to Atlantic cod (*Gadus morhua*). Variables and parameters without dimension are denoted '–' in the unit column.

2.2. Neutral buoyancy

A submerged fish has neutral buoyancy when it displaces a volume of water with a mass equal to its body mass (Archimedes' principle). The volume of a swimbladder giving neutral buoyancy (V_n; m^3) to a fish with body mass M (kg) can then be calculated given the density of the fish tissue (ρ_f; $kg\,m^{-3}$) and the density of water (ρ_w; $kg\,m^{-3}$):

$$V_n = \frac{M(1 - (\rho_w/\rho_f))}{\rho_w} \quad (1)$$

both ρ_w and ρ_f can be modelled as variables to reflect heterogenic environments and ontogenetic and seasonal changes for the particular species (discussed in e.g. Ona, 1990).

The amount of gas (mol) in the swimbladder was calculated using Boyle's law (Harden Jones, 1951; Alexander, 1959). If the actual swimbladder volume (V_s; m^3) differs from V_n, the fish will experience positive or negative buoyancy force (B; N):

$$B = (V_s - V_n)\rho_w g \quad (2)$$

where g is the gravitation constant ($9.81\,m\,s^{-2}$).

2.3. Swimbladder leakage

A swimbladder will need constant refilling due to diffusion into surrounding tissues (Denton et al., 1972; Lapennas and Schmidt-Nielsen, 1977; Ross, 1979). Oxygen diffusion is dependent on three variables: the oxygen permeability of the swimbladder wall, which again is dependent on its species-specific guanine and lipid content (Denton et al., 1972; Wittenberg et al., 1980); the swimbladder surface area (S_s; m^2); and the pressure gradient between the swimbladder and surrounding tissues ($P - P_0$; atm). The swimbladder of a general teleost is assumed to be formed as a prolate (cigar-shaped) ellipsoid with polar radius a (m) and equatorial radius b (m). The swimbladder surface is calculated based on the current swimbladder volume (V_s) and a and b ($a = ((V_s 3(a/b)^2)/(4\pi))^{1/3}$ when the ratio a/b is known):

$$S_s = 2\pi b^2 \left(1 + \frac{(a/b)\arcsin(e)}{e}\right) \quad (3)$$

where e (dimensionless) is the eccentricity of the ellipse given by $e = \sqrt{(1 - b^2/a^2)}$. Hence, the rate at which oxygen leaks from the swimbladder (Leakage; $mol\,s^{-1}$) is:

$$\text{Leakage} = \frac{GS_s(P - P_0)}{RT} \quad (4)$$

where G ($m^3\,O_2\,m^{-2}\,atm^{-1}\,s^{-1}$) is the oxygen conductance of the swimbladder wall, R ($m^3\,atm\,mol^{-1}\,K^{-1}$) the universal gas constant, and T (K) the temperature in Kelvin.

2.4. Secretion

The equations for gas secretion are based on work by Harden Jones and Scholes (1985). It is assumed that the diffusion barrier between the gas gland and the swimbladder is so little that the rate-limiting step is the transport of oxygen and multiplication of partial pressures in the rete and the gas gland. As a consequence, secretion will be independent of depth. The model calculates the maximum rate of secretion (Sec_{max}; $mol\,s^{-1}$), as a function of cardiac output (C_{out}; $m^3\,s^{-1}$), the fraction of C_{out} diverted to the *rete* (C_{rete}; dimensionless) (Pelster and Scheid, 1992), the volume fraction of O_2 in arterial blood (O_{2a}; dimensionless) measured at P_0 (1 atm), and an efficiency factor of the *rete* (R_{eff}; dimensionless):

$$Sec_{max} = \frac{C_{out}C_{rete}O_{2a}R_{eff}P_0}{RT\delta_{O_2}} \quad (5)$$

where δ_{O_2} is the fraction of oxygen in the secreted gases. It is likely that both C_{out} and C_{rete} vary in a complex fashion. At high exercise levels, it is likely that the *rete* experiences a reduction in blood flow as the exercising muscles are given priority. Similarly, at low activity levels, it is possible that the fish can increase C_{out}, and thus blood flow to the *rete*, when it needs to speed up absorption or secretion. Therefore, a static C_{out} estimated for a typical cruising speed combined with a static C_{rete} as the maximum measured value will give a good approximation of maximum blood flow and thus maximum secretion rate.

The minimal amount of work (W; J) required to isothermally compress (i.e. at constant temperature) one mol of gas at temperature T from pressure P_1 to pressure P_2 is (Glasstone and Lewis, 1964):

$$W = RT\ln\left(\frac{P_2}{P_1}\right) \quad (6)$$

It is further necessary to divide the minimum energy with an efficiency factor for converting biological chemical energy into mechanical energy (E_{eff}, dimensionless). E_{eff} includes the effects and energetic costs for the Bohr, Root, and salting-out effects, production of lactate, and the pentose-phosphate pathway (Pelster et al., 1989, 1994). If these effects were to be modelled explicitly, it would be necessary to know the cost and contribution of each of these effects. A precise set of equations to describe these processes thus requires further experimental research; in this model the focus is set on the overall energetic cost of secretion. E_{sec} (J s^{-1}) is thus the required energy to secrete the gases:

$$E_{\text{sec}} = \text{Sec}\, RT\, \ln\left(\frac{P}{P_0}\right) E_{\text{eff}}^{-1} \tag{7}$$

where P is the hydrostatic pressure and P_0 the combined partial pressures of the gases in arterial blood, assumed constant (1 atm). Sec is the amount of gases secreted and always less than or equal to Sec_{max}. The depth at which the leakage rate equals the maximum gas secretion rate is termed the critical depth (z_{c}; m), and was calculated by finding the pressure at which leakage from Eq. (4) equals maximum secretion from Eq. (5) ($P = 1 + z/10$):

$$z_{\text{c}} = 10\frac{\text{Sec}_{\text{max}} RT}{G S_{\text{s}}} \tag{8}$$

2.5. Absorption

Physoclist fish have a particular area on the swimbladder wall called the oval, which is specialised for gas absorption (Fänge, 1953; Steen, 1963b). There are three major variables that influence the rate of oxygen absorption (Steen, 1963b). First, only the fraction of the cardiac output that flows through the oval (C_{oval}; dimensionless) can absorb oxygen. Second, the pressure gradient between the swimbladder and the arterial blood (in this model calculated as $P - P_0$) determines the amount of gas that can be physically dissolved. Third, available oxygen-binding sites on haemoglobin can transport additional oxygen. By adopting the method of Harden Jones and Scholes (1985), the maximum oxygen absorption rates (Abs_{max}; mol s^{-1}) can be calculated as:

$$\text{Abs}_{\text{max}} = \frac{C_{\text{out}} C_{\text{oval}} P_0}{RT}\left[\frac{\text{O}_{2\text{sol}}(P - P_0)}{\delta_{\text{O}_2}} + O_{2\text{a}}\,\Delta\text{Hb}\right] \tag{9}$$

where $\text{O}_{2\text{sol}}$ the solubility of oxygen ($\text{m}^3\ \text{O}_2\ \text{m}^{-3}$ blood atm^{-1}) and ΔHb is the fraction of available haemoglobin binding sites (dimensionless). The δ_{O_2} includes the other gases that follow physically dissolved oxygen.

2.6. Hydrodynamic lift

When neutral buoyancy cannot be achieved by the swimbladder alone, lift (up or down) has to be created by hydrodynamic forces in order to avoid sinking or floating. Experimental studies have shown that large cod, by using their pectoral fins as hydrofoils while swimming freely, can compensate for 70–90% of the lift from the swimbladder (Ona, 1990). This model considers four distinct methods to create hydrodynamic lift: hovering without moving through the water, body lift, changing the tilt angle, and using the pectoral fins as hydrofoils. Hovering requires that the fish is stationary and cannot be combined with the other methods for hydrodynamic lift. The last three methods require that swimming speed and tilt angle are calculated simultaneously to find the most energy-efficient way to produce the required lift. An overview over the hydrodynamic forces considered is shown in Fig. 1.

The energetic cost of lift production has to be added to the standard metabolic rate SMR (J s^{-1}). The total metabolic rate (TMR; J s^{-1}) will then be either:

$$\text{TMR} = \text{SMR} + \text{MR}_{\text{HOVER}} + E_{\text{sec}} \tag{10a}$$

if the fish is hovering, and where MR_{HOVER} (J s^{-1}) is the metabolic cost of waving the pectoral fins; or:

$$\text{TMR} = \text{SMR} + \text{AMR} + \text{MR}_{\text{PECT}} + E_{\text{sec}} \tag{10b}$$

if the fish is swimming. AMR (J s^{-1}) is the energetic cost of swimming and MR_{PECT} (J s^{-1}) is the additional cost of lift production via the pectoral fins. AMR is equivalent to measured metabolic rate during swimming minus the standard metabolic rate. For a fish that beats a pair of fins of length F_{L} (m) through an angle γ to create a force equal to the buoyancy, the metabolic cost will be (Alexander, 2003):

$$\text{MR}_{\text{HOVER}} = \text{H}_{\text{GROUND}}\sqrt{\frac{|B|^3}{2WF_{\text{L}}^2\gamma}} \tag{11}$$

H_{GROUND} (dimensionless) is a factor that includes the energetic saving that can be obtained if hovering

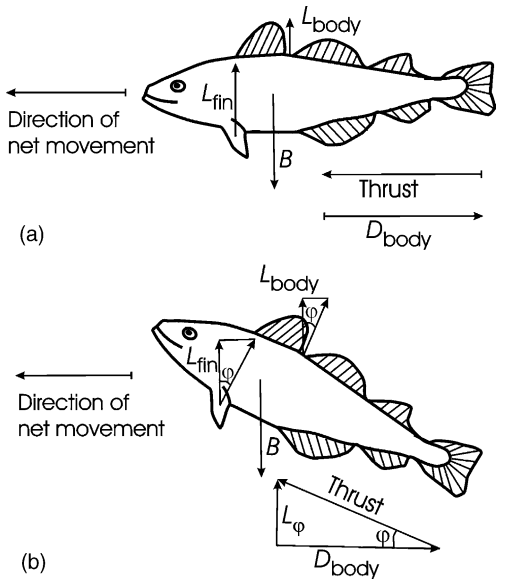

Fig. 1. Schematic drawing of the forces acting on a fish with swimbladder. (a) The forces acting on a negatively buoyant fish swimming horizontally. Thrust will equal drag at constant velocity. Lift is created by using the pectoral fins as hydrofoils (L_{fin}) and by the general body surface (L_{body}). (b) When the fish is tilting, the thrust vector can also produce lift (L_α). This will also affect the efficiency with which the pectoral fins and the body can create lift.

takes place close to the bottom (less than the length of the pectoral fins above solid substrate; (Blake, 1979). H_{GROUND} takes a value <1 when the fish is negatively buoyant and close to the bottom and 1 for all other situations. Blake (1979) calculated potential savings in the range 30–60% for the mandarin fish *Synchropus picturatus*. We have assumed that hovering is a potential option only for negatively buoyant fish.

The fish can also change its tilt angle φ. The *Thrust* (N) will then have a vertical component, which will give a lift L_φ (N):

$$L_\varphi = \sin\varphi\,\text{Thrust} \tag{12}$$

To find the thrust vector, we use the relationship power = force × velocity. Since power here is equal to the metabolic rate associated with swimming, we have:

$$\text{Thrust} = \frac{\text{AMR}\,\Omega}{U} \tag{13}$$

where U (m/s) is the swimming speed that the fish would have had if neutrally buoyant and swimming with the same metabolic cost. When the fish is tilting, part of the thrust vector is directed downward, and the horizontal velocity, which is the fish' speed through the water that can generate other types of lift, will be $U_H = \cos\varphi\, U$. A closer inspection of available literature on the metabolic cost of swimming revealed that swimming efficiency increased with swimming speed (e.g. Sepulveda and Dickson, 2000; Dickson et al., 2002; Nauen and Lauder, 2002). It was necessary to introduce the factor Ω (dimensionless), which is the biological efficiency of converting chemical energy to a propelling force. It is here modelled as a function of U^2 (reasons for the parameter Ω and its mathematical formulation are given in Section 4):

$$\Omega = \Omega_{\min} + \left(\frac{\Omega_{\max} - \Omega_{\min}}{U_{\max}^2}\right)\left(\frac{U}{\text{BL}}\right)^2 \tag{14}$$

where $\Omega_{\min}$ and $\Omega_{\max}$ are minimum and maximum values for Ω, respectively, and $U_{\max}$ is the maximum sustained swimming speed measured in BL s^{-1}. Typically, Ω would scale between $\Omega_{\min} = 0.05$ and $\Omega_{\max} = 0.20$. Defining Ω in this way preserves D_{body} as a function of $U^{2–2.5}$, and lets Ω scale with body size in accordance with the biological interpretation. For most species $U_{\max}$ decreases with body size and increases with temperature.

Given that the fish maintains a constant speed, the horizontal component of the thrust vector will be equal to the body drag D_{body} (N):

$$D_{body} = \cos\varphi\,\text{Thrust} \tag{15}$$

Many fish utilize also the body drag to produce lift, e.g. through having a dorsal curvature that gives the overall body a wing shape, or by specifically designed appendages. Holding the lift from the pectoral fins aside, we define body lift L_{body} (N) as the non-reversible (always working only upward) lift from the body:

$$L_{body} = \left[\frac{L}{D}\right]_{body} D_{body}\,\cos\varphi \tag{16}$$

where $\left[\frac{L}{D}\right]_{body}$ is a positive lift-to-drag coefficient for the body as a whole. A perfectly designed fin can have lift-to-drag coefficients up to 5 (Alexander, 1971), but the value for the whole body will for most fish be substantially lower. Note that since D_{body} is always positive, L_{body} will also be a non-negative value.

The pectoral fins can be extended as hydrofoils, which will increase the drag but also be very efficient at producing lift. We assume that the pectoral fins become less efficient at producing lift when the tilt angle increases; $L_{\text{fin}}/\cos\varphi$ is therefore used in the equation. The extra energy required to produce L_{fin} (N) lift is then (Alexander, 1990, 2003):

$$\text{MR}_{\text{PECT}} = \frac{(L_{\text{fin}}/\cos\varphi)^2}{\Omega\pi\rho_{\text{w}}U_{\text{H}}F_{\text{L}}^2} \tag{17}$$

The number 4 in the denominator in Alexander's original equation is cancelled by our use of fin length F_{L}, which is only half the span of the pectoral fin hydrofoil and when squared produces a 4 also in the numerator.

We now assert that the vertical forces have to sum to zero:

$$B = L_{\varphi} + L_{\text{body}} + L_{\text{fin}} \tag{18}$$

The best combination of tilt angle φ and swimming speed U can now be iterated from the set of equations by minimizing the sum of AMR and MR_{PECT}. The resulting cost of swimming to create hydrodynamic lift can then be compared to the energetic cost of hovering to see which option is favourable in energetic terms.

2.7. An example: Atlantic cod

To test this description of buoyancy control, the model was parameterised for Atlantic cod (*G. morhua*). For some parameters, experimental values had not been obtained for cod, and we were forced to use values from other species. In a model as complex as this one, there will necessarily be biological parameters not yet experimentally determined. For this reason, emphasis was put on matching the overall output from the model's different components with data where available, and uncertain parameters were tuned against experimental studies on cod swimbladder dynamics and swimming physiology (e.g. Tytler and Blaxter, 1973; Harden Jones and Scholes, 1985; Sepulveda and Dickson, 2000). To help visualize the sensitivity of the predicted output from the model, many of the results are plotted for fish of various sizes and over a wide range of swimbladder volumes.

A value of 1081 kg m^{-3} was used for cod tissue density (Harden Jones and Scholes, 1985). Based on X-ray pictures of cod (Clay and Horne, 1994), the length to width ratio (the a to b ratio in Eq. (3)) was estimated to be 10. Scholander (1956) found that O_2 made up on average 63% of the secreted gases in cod, thus $\delta_{O_2} = 0.63$. The energy converting efficiency during secretion was set to $E_{\text{eff}} = 0.10$ (Alexander, 1971). The oxygen content of arterial fish blood was set to 10% by volume ($O_{2a} = 0.10$, Prosser, 1973; Harden Jones and Scholes, 1985). Steen (1963a) obtained experimentally a *rete* efficiency of 20% in the eel (*Anguilla anguilla*), thus $R_{\text{eff}} = 0.20$. These parameters describe secretion in accordance with the experiments in Harden Jones and Scholes (1985).

The total metabolic cost (TMR; Eq. (10b)) was calculated based on a general bioenergetic model by Hewett and Johnson (1992) with cod parameters (Hansson et al., 1996):

$$\text{SMR} = \alpha M^{\beta} F(T) \tag{19a}$$

$$\text{AMR} = \text{SMR}\,\text{Act} \tag{19b}$$

$$\text{Act} = \frac{3.2U^{1.5}}{\text{BL}} \tag{19c}$$

where αM^{β} is a weight dependent and $F(T)$ a temperature dependent function of metabolism with $\alpha = 0.397$, $\beta = 0.828$, and $F(T) = 0.502$ at 5 °C (see Hansson et al., 1996 for details). Act (dimensionless) is the incremental cost of activity and is estimated based on measurements of oxygen consumption during swimming (U) for cod in the range 0.24–1.91 kg (expressed on the form used in Ware, 1978; Schurmann and Steffensen, 1997; Webber et al., 1998; Reidy et al., 2000).

Cardiac output (C_{out}, $\text{m}^3\,\text{s}^{-1}$) based on data from Webber et al. (1998) was calculated as a function of body mass and the metabolic rate corresponding to a cruising speed of 0.4 BL s^{-1}:

$$C_{\text{out}} = 9.07 \times 10^{-7}\text{TMR} - 3.79 \times 10^{-8}M \tag{20}$$

Pectoral fin length (F_{L}) was calculated from body length (BL) using a relationship obtained for cod ranging from 10 to 105 cm (based on unpublished data from A.G.V. Salvanes; $n = 400$, $R^2 = 0.98$):

$$F_{\text{L}} = 0.1374\text{BL} + 0.0039 \tag{21}$$

Following Alexander (2003), the angle through which the fin beats when hovering was set to $\gamma = \pi$ radians. Maximum sustainable swimming speed (U_{max}; BL s^{-1}) was modelled to fall from 1.8 BL s^{-1} in 0.2 kg

cod and stabilise at 1.2 BL s^{-1} in cod > 3 kg (based on data from Schurmann and Steffensen, 1997; Webber et al., 1998; Reidy et al., 2000):

$$U_{max} = 0.8e^{-M} + 1.2 \quad (22)$$

The parameters G (the oxygen conductance of the swimbladder wall), C_{rete}, and C_{oval} (the proportion of cardiac output that can be directed to the rete and the oval, respectively) have to our knowledge not been measured for cod. Harden Jones and Scholes (1985) measured rates of absorption and secretion in cod, and these parameters were chosen to match their experimental results. The blood flow to the oval (C_{oval}) was measured in anaesthetized eel (*Anguilla vulgaris*) by Steen (1963b) and found to be in the range 6–28%. C_{rete} has to our knowledge not been measured. Since the *rete* with its counter-current vascular structure is much more elaborate than the oval, we used $C_{oval} = 0.25$ and $C_{rete} = 0.10$, two values that provided good fit with the experimental data on cod from Harden Jones and Scholes (1985). Lapennas and Schmidt-Nielsen (1977) measured oxygen conductance G between 1.5×10^{-9} and 1.5×10^{-8} m^3 O_2 m^{-2} atm^{-1} s^{-1} in the deep-dwelling Conger eel (*Conger oceanicus*) and five teleosts utilising shallower habitats compared to cod. A value in the lower range, $G = 1.5 \times 10^{-9}$, was chosen so that a 2-kg cod would have a critical depth $z_c \approx 533$ m. The model's predictions of net secretion rates and critical depths are sensitive to the numerical value of G; any choice of G should therefore be accompanied by comparisons of critical depths with the species' vertical distribution. Cod is regularly found down to depths of 400 m (Godø and Michalsen, 2000), and because secretion (by volume) is very slow close to the critical depth, our choice of G implies that the cod over its entire vertical range has a swimbladder that responds to depth change within reasonable time (Fig. 2a). Data on ontogenetic changes in the gas conductivity of swimbladder wall tissue has, to our knowledge, not been published. Gas conductivity was therefore assumed constant in this model.

We assumed $\left[\frac{L}{D}\right]_{body} = 0.75$, which is the conversion of drag over the fish body to a vertical lift component (discussed in Vogel, 1994, pp. 239–240); the parameter has to our knowledge not been determined for fish). This included lift produced by the overall body surface and body shape, and resulted in a slight asymmetry in the energetic cost between creating positive and negative lift.

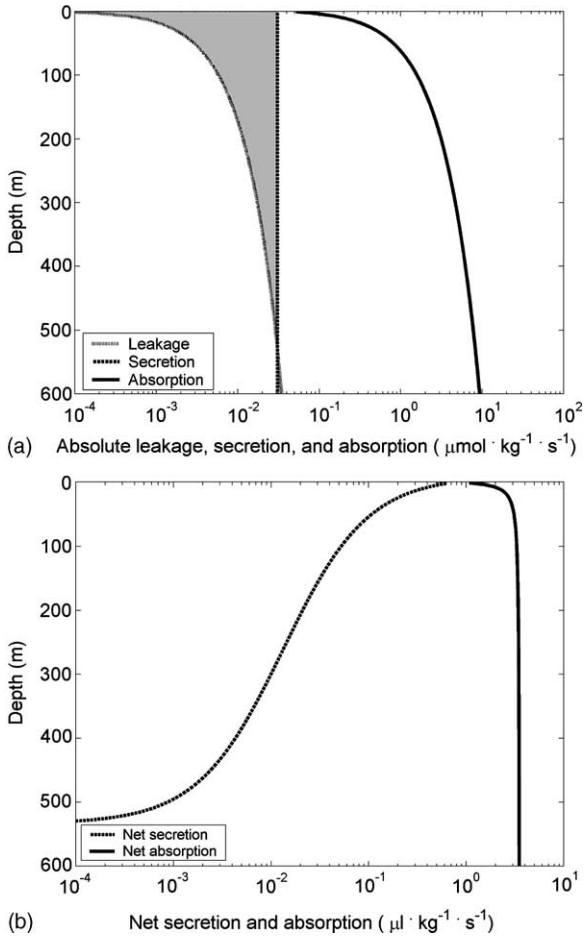

Fig. 2. Swimbladder dynamics as a function of depth in a model parameterised for cod *Gadus morhua*. (a) Absolute leakage (dotted line), secretion (dashed line), and absorption (solid line) as a function of depth, expressed in (μmol kg^{-1} s^{-1}). The grey area is the difference between leakage and maximum secretion and is thus the maximum net secretion possible at that depth, (b) Net secretion and absorption, both including the effects of leakage, measured in volume (μl kg^{-1} s^{-1}). The calculations were made for a 2-kg Atlantic cod. Note the log x-axes.

To our knowledge, no study has ever combined measures of different aspects of buoyancy regulation to a degree that can be used as a set of independent data to validate the model described above. That would require simultaneous measures of gas rates, buoyancy, swimming speed and mode, and metabolic rate. Rather,

swimbladder dynamics and hydrodynamic lift generation has to be tested separately against experimental datasets, and the combination of the two in a bioenergetic framework can at present only be shown, not tested. To compensate this, we have tried to use parameter values from published experiments and strived to make our thoughts and assumptions as clear to the reader as possible. We have also taken two approaches to demonstrating the benefits from combining swimbladder dynamics and hydrodynamic lift generation. First, we show estimates for the energetic cost of buoyancy control for a series of constructed patterns for diel vertical migration for a 2-kg cod. Each migration pattern was simulated for 6 days to stabilize, and results were shown for the last 24-h period only. Second, we visualise the model using 12 months of data on vertical positions collected from a 3-kg cod carrying a data storage tag (resolution 2 h, interpolated to time-steps of 15 min, from Godø and Michalsen, 2000). The cod was tagged on the 21 March 1996. To assure that any possible handling wounds would have healed, three weeks, starting at 22 October 1996, were selected for visualisation.

3. Results

Several authors have studied different modes of buoyancy regulation (e.g. Steen, 1963a; Alexander, 1972; Harden Jones and Scholes, 1985; Vogel, 1994). The results presented here provide the basics of the different modes, but focus on the link between swimbladder dynamics and hydrodynamics made possible in our paper by the common bioenergetics approach. It is in the linking of the different modes of buoyancy regulation in a common currency that our work transcends earlier work and creates a basis for future behavioural models and field data interpretation.

3.1. Swimbladder dynamics

The swimbladder is subject to the physical laws for gases, which make swimbladder dynamics dependent on both depth and body size. To clarify the picture, we will describe how rates, in mol s^{-1}, vary with depth, and then focus on how this is translated into volume changes and affect the behavioural repertoire.

The processes that describe leakage and absorption of gases from the swimbladder depend on the difference in partial pressure between the swimbladder (at hydrostatic pressure) and the surrounding tissues including blood (in equilibrium with sea surface conditions at best). As this pressure difference increases with depth, the rates for these two processes will also increase (Fig. 2a). The absolute gas secretion rate is, on the other hand, unaffected by depth (Fig. 2a). Consequently, the net rate of gas secretion, which is how fast the swimbladder can be filled, decreases with depth (the shaded area in Fig. 2a). Note that these rates are maximum rates, and we assume full regulatory flexibility within these limits.

The pattern of volume changes is different from secretion and absorption rates, due to the increasing hydrostatic pressure with depth (Fig. 2b). Although more gas molecules (measured in mol) can be absorbed with depth, the volume that can be absorbed is almost independent of depth except for slow changes close to the surface. Overall, the volume that can be absorbed is much larger than the volume that can be secreted per unit time (the axis in Fig. 2b is logarithmic; absorption volume is 10–10,000 times larger than the secretion volume depending on depth). Maximum net secreted volume declines rapidly with depth and approaches zero where leakage and secretion rate cancel each other. This asymmetry between absorption and secretion means that fish will more often be negatively than positively buoyant (noted by Alexander, 1966; Tytler and Blaxter, 1973; Arnold and Greer Walker, 1992). In addition, filling the swimbladder is radically slower at greater depths, which will affect the costs and benefits of vertical behaviour.

Harden Jones and Scholes (1985) present to our knowledge the best experimental data set on absorption and secretion in cod. We have carefully chosen the parameter values of C_{rete} and C_{oval} so that the swimbladder dynamics of our model match their data within $\pm 10\%$ over the range of depths included in their study. Our estimates are also very similar to those obtained experimentally by Tytler and Blaxter (1973). Because the surface:volume ratio decreases with increasing size, a larger fish will have a relatively lower gas leakage across the swimbladder wall. As a result, critical depth increases with body size (Fig. 3).

Energy is required to pressurise gases in the blood to fill the swimbladder. When gas secretion

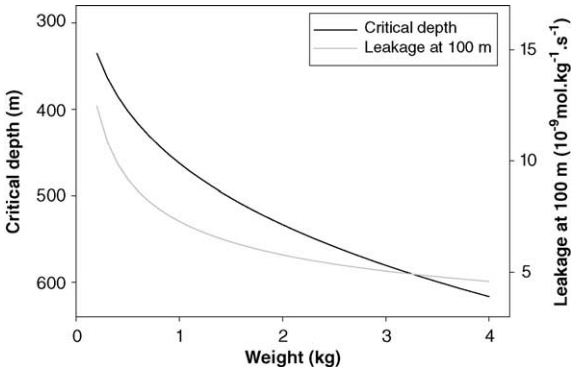

Fig. 3. Size dependence of critical depth and leakage across the swimbladder wall. The surface-to-volume ratio of the swimbladder changes as a cod grows in size. As an effect, the relative amount of gas leaking across the swimbladder wall decreases with body size (grey line). Critical depth, i.e. the depth at which maximum secretion equals gas leakage, will thus increase with body size (black line).

is at its maximum, the estimated energetic cost is $0.0017\,\mathrm{J\,kg^{-1}\,s^{-1}}$. This corresponds to 1.0% of the standard metabolism and is, as will be shown below, close to negligible compared to the energy required for swimming.

3.2. Hydrodynamic lift

If neutral buoyancy can not be achieved through the swimbladder alone, the fish must depend on hydrodynamic lift to maintain its position in the water column. The present model assumes that lift is produced either by hovering, or by swimming at the optimal tilt angle, which would combine pectoral fin lift, body lift, and lift from the tilted thrust vector. Lift created by hydrodynamic forces is independent of depth. We will present results for fish of varying body mass, and for lift production corresponding to swimbladder volumes ranging from −100% (empty swimbladder) to +100% (double size) of the optimal volume. We will first focus on hydrodynamic lift created during swimming, before we turn to hovering as an alternative and compare the two.

The more the swimbladder volume deviates from the optimal volume, the higher was the estimated compensatory swimming speed (Fig. 4a). The compensatory swimming speed also increased with fish size when measured in $\mathrm{m\,s^{-1}}$, but when measured in $\mathrm{BL\,s^{-1}}$ it did not vary with body mass. Each half of Fig. 4a had the

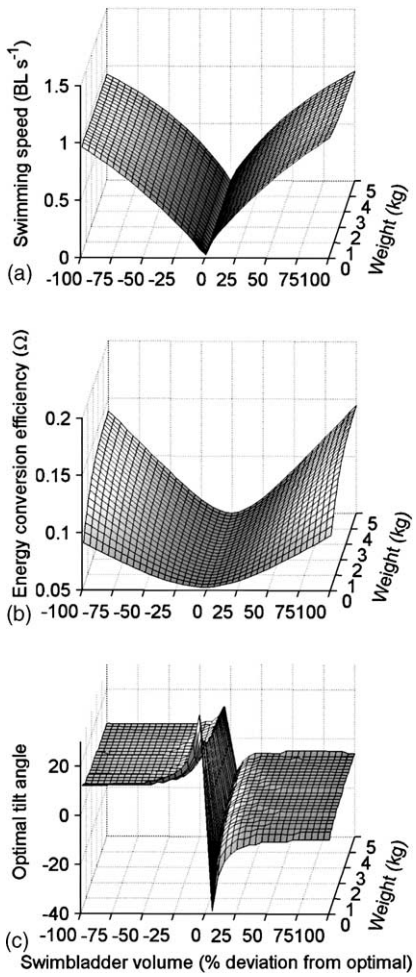

Fig. 4. Properties of hydrodynamic lift production when the swimbladder volume deviates from optimal. The left-to-right axis is the swimbladder volume, where 0% corresponds to the optimal volume that would have resulted in neutral buoyancy. Negative buoyancy (sinking) is to the left; positive buoyancy (floating) to the right. Fish size (kg) increases from 0.2 kg in front to 5.0 kg in the back. (a) Compensatory swimming speed, expressed in body lengths per second ($\mathrm{BL\,s^{-1}}$). (b) The values taken by the energy conversion efficiency Ω between the fish' oxygen consumption and the physical work required to overcome drag. Ω increases with increasing swimming speeds up to maximum sustainable swimming speed, where it would reach a maximum of 0.20. (c) The optimal tilt angle at different levels of buoyancy and fish size. Panels (a) and (b) assume that the fish was swimming at the optimal tilt angle.

expected concave-up shape: the deviation in swimbladder volume is proportional to the required lift, which is proportional to drag, which again is a function of U^{2-3}. This was achieved by the energy conversion efficiency

Ω (Fig. 4b), which scales with swimming speed from 0.05 (at zero swimming speed) to a maximum value of 0.20 (at the maximum swimming speed; see Section 4 for details).

Close to neutral buoyancy, fish will have a low energy conversion efficiency Ω. They will therefore use relatively more energy for swimming at the speed that creates sufficient drag for lift production, which in turn will favour a steeper tilt angle (Fig. 4c). The optimal tilt angle increased also for small fish. This is because smaller fish have a higher maximum sustainable swimming speed (Eq. (22)) and will hence achieve a relatively lower energy conversion efficiency Ω. For most combinations of size and buoyancy, the optimal tilt angle was found to be around 7° for both positive and negative buoyancy.

For lift produced by compensatory swimming, the energy expenditure, measured per kg body mass, was strongly dependent on the experienced buoyancy, but showed little variation between fish of different size (Fig. 5a). The asymmetry between negative (left half) and positive (right half) buoyancy seen in Fig. 5a is due to body lift. Body lift will always work towards the surface due to the shape of the fish, irrespective of the buoyancy force experienced by the fish. Whenever the fish is negatively buoyant, body lift will reduce compensatory swimming speeds and thus also energy requirements, while the opposite effect takes place during positive buoyancy.

The energetic cost of hovering is shown in Fig. 5b. In our model, hovering is only possible when the fish is negatively buoyant. The energetic cost of hovering rose sharply with the degree of underflotation and with increasing body size. Because the energy consumption during compensatory swimming was a concave-down function and that for hovering concave-up, hovering was energetically preferential when the fish was only slightly negatively buoyant (Fig. 5c). Hovering was also more often the best option for smaller fish. Small fish, experiencing close to neutrally buoyancy, gain most from tilting compared to fish orientated hor-

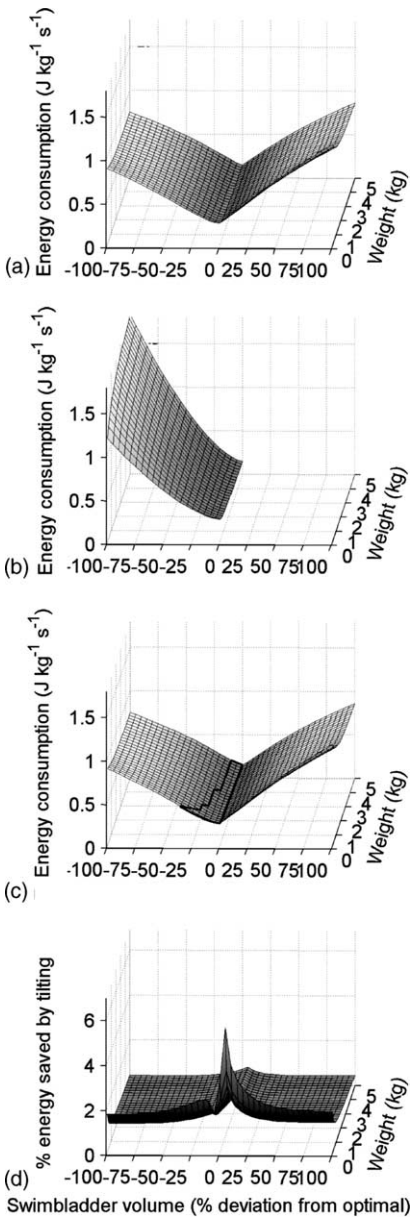

Fig. 5. Energy consumption for different modes of hydrodynamic lift production. The left-to-right axis is the swimbladder volume, where 0% corresponds to the optimal volume that would have resulted in neutral buoyancy. Negative buoyancy (sinking) is to the left; positive buoyancy (floating) to the right. Fish size (kg) increases from 0.2 kg in front to 5.0 kg in the back. The calculations assume that the fish were swimming at the optimal tilt angle. The graphs show energy expenditure (J kg^{-1} s^{-1}) to produce the required lift by means of (a) hydrodynamic lift by swimming with the pectoral fins extended, (b) standing still hovering, and (c) the most energy-efficient combination of pectoral fins and hovering. The area where hovering is beneficial is indicated by the thick black line. Panel (d) shows how much energy fish gain from applying the optimal tilt angle (see Fig. 4c) compared to orientating the body horizontally (tilt angle = 0°). See text for details.

izontally (in percentage change between tilting and non-tilting) (Fig. 5d). Larger fish gain relatively less than small fish independent of buoyancy level. However, the absolute amount of energy saved by tilting (kJ kg^{-1} s^{-1}) increases for all size classes with both decreasing and increasing buoyancy.

3.3. Ecological implications

Hydrodynamic forces stemming from swimming and lift from the swimbladder often complement each other in producing lift; the swimbladder being slow to adjust but energetically cheap to operate while hydrodynamic forces have the opposite properties. To show how these two modes of lift production work together, we show the estimated energetic cost for various vertical migration patterns in Fig. 6. The example assumes that cod stayed at 200 m depth during daytime and migrated to shallower waters during the night to feed (this behaviour is representative for cod, see e.g. Godø and Michalsen, 2000). The vertical movement was set to take always 1 h, so that 11 h were spent at the top and the bottom of the vertical range (examples are shown in Fig. 6a). Because gases are absorbed much faster than they are secreted, the cod was close to neutrally buoyant at the top of the vertical range. At the daytime depth, cod became progressively more negatively buoyant as the vertical migration distance increased (Fig. 6b). Consequently, hydrodynamic forces had to compensate for negative buoyancy through increased swimming (Fig. 6b), and the energetic cost increased rapidly with increasing vertical migration distance (Fig. 6c). During night, fish that stay closer to the surface experience a lower leakage and hence cheaper maintenance of the optimal swimbladder volume, which is the reason that the energetic cost fall with migration distance (Fig. 6c).

3.4. Application to field data

The model predictions were further explored by applying it to a set of observed vertical positions of an individual cod recorded over one year using a data storage tag (Godø and Michalsen, 2000, Fig. 7a). Only a subset of three weeks starting 22 November 1996 is presented. It was assumed that the fish had neutral buoyancy at the start of the period and the first simulated day is not shown to allow the simulated swimbladder volume

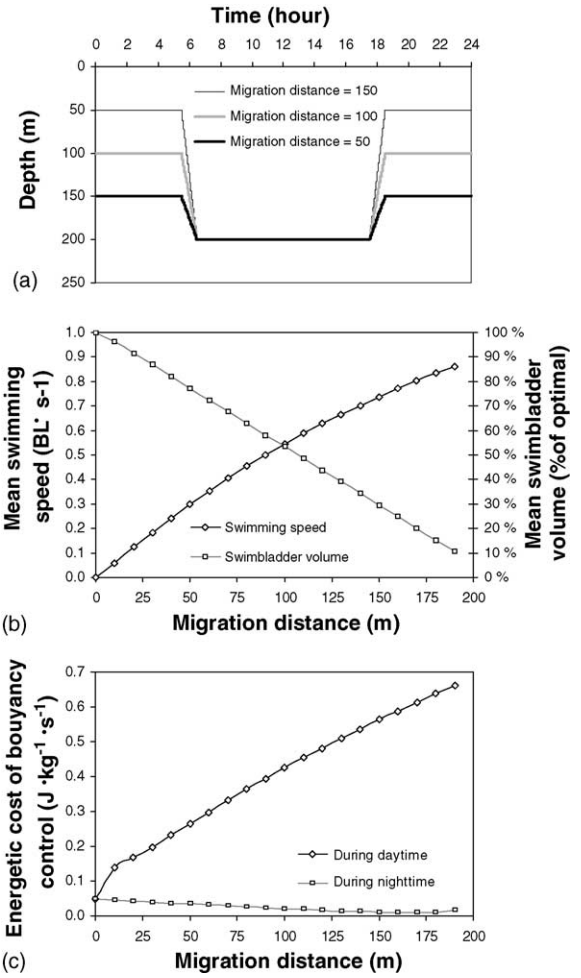

Fig. 6. A constructed example of diel vertical migration in cod and the corresponding predictions of swimbladder volume, swimming speed and energetic cost from a model paramterised for cod *Gadus morhua*. (a) Examples of constructed diel vertical migration patterns for which buoyancy regulation were simulated for a 2-kg cod. The pattern was simulated for 6 days to stabilise; only the results for the last 24-h period are shown, (b) Mean swimbladder volume and compensatory swimming speed to create the required lift at the daytime depth as a function of the vertical migration distance. At the top of the vertical range, swimming speed was close to zero and the swimbladder volume virtually optimal, (c) The energetic cost of buoyancy regulation separated by the periods spent at the bottom (day) and top (night) of the vertical migration profile.

to stabilize. The model was not sensitive to the choice of initial swimbladder volume. Estimated swimbladder volumes were between −40 and 0% deviation from optimal volume (Fig. 7b). Calculated energy expenditure,

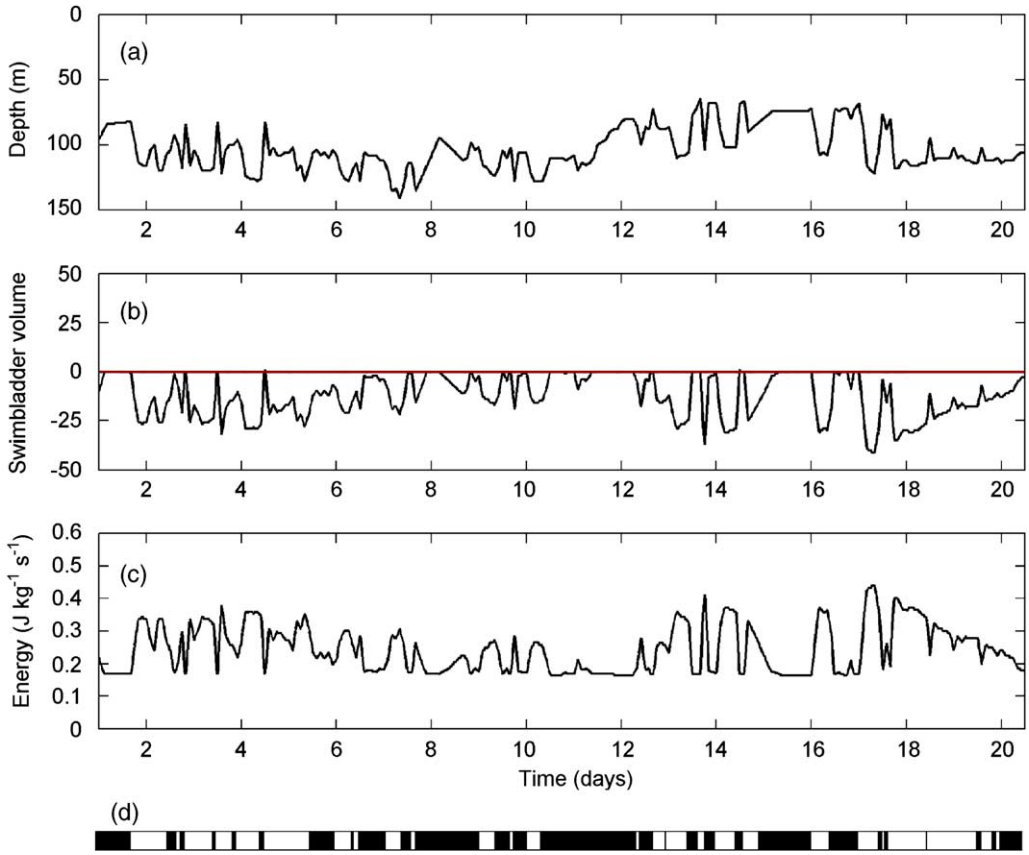

Fig. 7. (a) The observed vertical position of one Atlantic cod over a period of three weeks (data from Godø and Michalsen, 2000). (b) The model's prediction of the cod's experienced swimbladder volume expressed in percent deviation from the optimal swimbladder volume that would have given neutral buoyancy. The cod was assumed to be neutral at time 0 and the first day is not shown to allow the swimbladder volume to stabilise. The horizontal line is optimal swimbladder volume. (c) The corresponding energy consumption (J kg^{-1} s^{-1}) due to standard metabolic rate, the cost of gas secretion, and activity metabolism caused by compensatory swimming speed when the swimbladder volume deviated from optimal. The standard metabolic rate (SMR) is identifiable as the baseline (swimbladder volume optimal and thus no need for compensatory swimming). (d) The black bars indicate when the model predicted that hovering would have been an energetically favourable option.

including secretion and compensatory swimming, is shown in Fig. 7c. The standard metabolic rate (SMR) is recognisable as the baseline for energy expenditure. Late on day 17, the cod went down to around 100 m and stayed there for several days with only short vertical migrations to shallower depths. The model estimated that secretion slowly filled the swimbladder, and predicted decreasing compensatory swimming speeds that would lead to a steady decrease in energy expenditure. After approximately 2 days, the swimbladder had attained optimal volume. Hovering was not enabled in this simulation, but the energetic cost of hovering was calculated for comparison. The black bars in Fig. 7d indicate when the model predicted that hovering would have been energetically favourable. As expected, hovering was only favourable when the fish was close to neutrally buoyant; in total 50% of the time.

4. Discussion

The presentation of this model is based on parameter values for cod. In a strict sense, the results apply only to cod. However, throughout this discussion of buoyancy regulation we try to establish a wider perspective, aiming at making general points with validity for a broad

range of fish species that have physoclist swimbladders. More precise predictions will require that the model is re-parameterised for the relevant fish species. It should be possible to apply an adjusted version of the model to some physostome fish by allowing the fish to expel air if it becomes positively buoyant. It is also unclear to what extent physostome fish are capable of secreting gas (Moyle and Cech, 1988; Nøttestad, 1998).

4.1. The swimbladder

There are complex changes in the available behavioural repertoire of physoclist fishes with increasing depth. For example, frequent vertical movements will lead to negative buoyancy because absorption is faster than secretion, an effect that is amplified on greater depths. This is mainly due to the fact that net gas secretion is reduced while gas absorption is faster with increasing depth. Ontogenetic differences also impact swimbladder characteristics in many ways. During growth, the surface to volume ratio of the swimbladder decreases. This reduces the relative gas leakage from the swimbladder, giving larger fish a comparative advantage at greater depths. To what extent such an ontogenetic shift is involved in shaping the vertical positioning strategies of different-sized fish is, however, difficult to estimate as so many other important aspects of evolution can affect behaviour (e.g. predation risk, food accessibility).

Note also that the rates calculated are maximum rates and that regulation takes place within the calculated limits, analogous to nervous control with physiological constraints. The swimbladder wall is provided with stretch receptors (Qutob, 1962) and innervated by the autonomous nerve system (Wahlqvist, 1985; Schwerte et al., 1997). Although this would imply that fish are unable to deliberately plan whether or not to secrete or absorb gas, it would instead allow fish to autonomously and continuously adjust their swimbladder volume towards neutral buoyancy with great flexibility within the calculated limits.

4.2. Negative versus positive buoyancy

First, it would be instructive to establish to what extent over- or underflotation occur in nature. Current interpretations of empirical data conclude that cod stays neutral near the top of its vertical range and becomes progressively more negatively buoyant at greater depths (Alexander, 1971; Harden Jones, 1981; Arnold and Greer Walker, 1992; Godø and Michalsen, 2000). This tendency towards negative buoyancy was also evident when the model was applied to constructed diel vertical migration patterns and field data. Calculations made on the observed behaviour from the tagged cod indicated that most of the time was spent with a swimbladder volume between −40 and 0% deviation from the optimal volume, and the cod was never significantly positively buoyant. With this in mind, our focus has been to model situations close to neutral buoyancy and with underflotation up to −40% as realistically as possible; the model thus sketches a coarser landscape of energy usage for the less used behaviours. The model also presupposes a physiologically intact swimbladder in all situations. If the swimbladder's functionality is compromised, e.g. by rupture during rapid ascents, certain limitations must be defined in the model.

A 2-kg cod that swims at a speed of 0.25 BL s^{-1}, which is the average swimming speed measured in free-ranging cod (due to e.g. food search, horizontal migrations) (Løkkeborg, 1998), would, without increasing its energy budget, be able to freely deviate within 89 and 106% of optimal swimbladder volume. Adapted to 100 m, this means that moving between 93 and 114 m would be without additional energetic costs. For a cod adapted to 300 m, this range would extend from 282 to 338 m.

Buoyancy can be both positive and negative, and creating a lift to overcome it may turn out to be different depending on whether the force has to be created up or down. Three aspects suggest that there is an asymmetry: (1) gas absorption is much faster than gas secretion. A fish is therefore likely to spend much more time negatively than positively buoyant, and should thus be most efficient at counteracting negative buoyancy. (2) The lift generated by a wing that moves through a medium is dependent among other factors on wing shape, surface area, and angle of attack (Vogel, 1994). Although the pectoral fins of cod are highly manoeuvrable in all directions, the posterior part of the fin base is positioned more ventrally than the anterior fin-base: this gives the fins a positive angle of attack. (3) Dorsal curvature and flattened fish bodies may also provide lift merely by moving forward through the water. This asymmetry is included in the parameter $\left[\frac{L}{D}\right]_{\text{body}}$, which

in a broad interpretation includes the effects of point 2 and 3 above. As a result, it is energetically cheaper to produce positive lift, which is the common situation since fish are most often negatively buoyant.

4.3. Energy conversion

There is a paradox in the way active metabolic rate scales with swimming speed that became apparent during the work trying to solve the equations for drag involved in this paper. Body drag is most likely to be proportional to $U^{1.5–2.0}$ (Vogel, 1994). Power is force × velocity, which means that active metabolic rate (AMR; $J\,s^{-1}$) required to overcome body drag at a given swimming speed, should be proportional to $D_{body} \times U$, i.e. proportional to $U^{2.5–3.0}$. Paradoxically, measures of metabolic rate at increasing swimming speeds show that metabolic rate is proportional to $U^{1.0–1.5}$, not $U^{2.5–3.0}$ (Schurmann and Steffensen, 1997; Webber et al., 1998; Reidy et al., 2000; Sepulveda and Dickson, 2000). This suggests that fish are more efficient in converting chemical energy into physical work at higher swimming speeds.

Digital particle image velocimetry can precisely measure the force exerted on water, and has recently been applied on swimming fish (e.g. Drucker and Lauder, 1999). For chub mackerel *Scomber japonicus* swimming at constant speed in a flow tunnel, thrust was found to be a function of $U^{2.5}$ (Nauen and Lauder, 2002). Metabolic rate should then be proportional to $U^{3.5}$. However, a regression on measurements of active metabolic rate in another study on chub mackerel revealed that metabolic rate was a function of $U^{1.1}$ (Sepulveda and Dickson, 2000; Dickson et al., 2002). A closer look on the data reveal that the ratio Ω between physical work per time (Nauen and Lauder, 2002) and metabolic rate (Sepulveda and Dickson, 2000) increased from 0.05 at 1.2 BL s^{-1} to 0.20 at 2.2 BL s^{-1}. Such an increased efficiency can explain the discrepancy between the theoretical and the measured relationships between AMR and U. We used lower swimming speeds for cod in our model since the chub mackerel is a faster swimmer, but the general observation that efficiency increases with swimming speed was preserved the way we modelled Ω. The biological interpretation of an increasing Ω may embody an enhanced efficiency as the number of recruited motor units increases, as well as the mechanisms by which elasticity can be brought into play by the undulating fish body. Ω would typically be higher in fish species well-adapted to prolonged or fast swimming.

4.4. Tilt angle

Tilting has strong implications for fisheries science because target strength changes with the exposed cross-sectional area of the swimbladder (MacLennan and Simmonds, 1992). Herring, for example, undertake extensive vertical migrations during overwintering, and these migrations are associated with large changes in tilt angle (Huse and Ona, 1996). Our results show that tilting could save energy, although our model predicted energy savings of only 0.5–6%. This is consistent with the relatively small optimal tilt angle of around 7° predicted by the model. Since tilting probably will be in conflict with common behaviours such as foraging, transport, and predator avoidance, it may be seen mostly during periods of rest or inactivity, or during overwintering as in the case of herring.

Another feature that changes target strength of fish is changes in swimbladder volume caused by vertical migration (Nakken and Olsen, 1977; Ona, 1990). This is a problem during acoustic abundance measurements of cod at times when the cod spends a considerable part of the day off the bottom (Rose and Porter, 1996). In such cases, the swimbladder volume and thus target strength (the acoustic reflection measured by an echosounder) will often be reduced deeper down since cod is usually neutrally buoyant at the top of the vertical range. Both tilt angle and swimbladder volume can significantly influence target strength. Our model provides predictions of swimbladder volume and tilt angle when the vertical behaviour is known. In combination with equations relating target strength to swimbladder volume or shape (e.g. Ona, 1990), these predictions can be used to improve estimates and uncertainties in biomass estimates.

This model considers hovering and using fins as hydrofoils (including body lift and changing the tilt angle) as the only alternatives to swimbladder regulation. Analogous to the effects of gait transitions on the energetic cost of terrestrial locomotion, more energetically feasible solutions may apply at different levels of under- or over-flotation. An alternative mode of buoyancy regulation is suggested by the sawtooth like profile sometimes seen during tracking of individual

fish on echograms. This pattern probably stems from voluntary floating/sinking interspersed with periods of more or less vertical swimming (Huse and Ona, 1996). Weihs (1973) suggested that a glide (downwards) and swim (upwards) mode of behaviour during horizontal migrations could be energetically advantageous for continuously underflotated fish, such as fish without swimbladders (e.g. *Scombrids*). This type of behaviour, however, is to our knowledge not reported for cod, but could be favoured in situations when fish experiences buoyancy outside its normal range, or when e.g. fast swimming required for hydrodynamic lift production would make the fish conspicuous to predators.

4.5. Interpretation of field data

The calculated swimbladder volumes and energy expenditure for the cod equipped with a data storage tag show how the present model can aid interpretation of observed behavioural patterns (Fig. 7a–d, Godø and Michalsen, 2000). The cod was likely to have foraged at times, and thus actively swimming more or less regardless of the state of its swimbladder throughout the period of recording. The predicted swimbladder volume dynamics and corresponding energy expenditure do not take other possible activities into consideration. Interestingly, the application of this model to observed depth positions opens up for a systematic analysis of the energetic implications of different categories of behaviour. Coupling this information with the knowledge of cod behaviour throughout the year and in different geographical areas can help us understand the ecological significance of these behaviours and also point towards the evolutionary motivation that has shaped them.

5. Conclusions

According to the resolution of the time scale, it is possible to use the equations described here to study behaviour in varying detail. Although the numerical estimates of energy consumption are to some degree uncertain, it will be possible to use the qualitative estimates to compare both behavioural strategies and geographical and temporal variations from longer time-series. In a more detailed perspective, the energetics during daily vertical migrations in combination with estimates of swimming speed can aid interpretation of actual and optimal behaviour.

The presented model makes explicit ways in which energetic costs and physiological constraints associated with buoyancy control influence on behaviour. The rapidly increasing hydrostatic pressure with depth affects how readily the swimbladder can accommodate to depth changes. As the swimbladder responds more slowly, compensatory swimming can create lift, but will also increase the overall cost of buoyancy regulation. The relative importance of the swimbladder and compensatory swimming will thus shift with depth, and the implications for behaviour will vary.

This model synthesises available information about the swimbladder and hydrodynamic buoyancy regulation. While some aspects of fish buoyancy regulation are well understood, it is evident that other aspects require more research. Especially, both experimental and theoretical studies of swimbladder volume during natural behaviour and the hydrodynamics of swimming including drag and lift are needed. The paradoxical relationship between metabolic rate and swimming speed suggests that metabolic efficiency increases with swimming speed. The crudely modelled efficiency factor Ω in this paper suggests a type of solution that may aid disentangling this complex relationship. The recent advances in thrust measures using digital particle image velocimetry (e.g. Drucker and Lauder, 1999) are promising and may provide a more accurate description of this phenomenon. However, the difficulties of scaling, where drag scales with absolute swimming speed while metabolism and elastic properties scale with body size, still push a mechanistic understanding into the future.

Acknowledgements

We would like to thank K. Michalsen for kindly providing us with the depth versus time data set on which we were able to visualise the model, A.G.V. Salvanes for data on fish fins, and I. Huse for reading and commenting the manuscript. We would also like to thank two anonymous reviewers for valuable comments. E.S. was supported by The Research Council of Norway and the European Commission contract Q5RS-2002-00813; C.J. and G.H. were supported by The Research Council of Norway.

References

Alexander, R.M., 1959. The physical properties of the swimbladders of fish other than Cypriniformes. J. Exp. Biol. 36, 347–355.

Alexander, R.M., 1966. Physical aspects of swim bladder function. Biol. Rev. Camb. Philos. Soc. 41, 131–176.

Alexander, R.M., 1971. Swimbladder gas secretion and energy expenditure in vertically migrating fishes. In: Farquhar, G.B. (Ed.), Proceedings of an International Symposium on Biological Sound Scattering in the Ocean. Maury Center for Ocean Science, Washington DC, pp. 74–85.

Alexander, R.M., 1972. The energetics of vertical migration by fishes. Symp. Soc. Exp. Biol. 26, 273–294.

Alexander, R.M., 1990. Size, speed and buoyancy adaptations in aquatic animals. Am. Zool. 30, 189–196.

Alexander, R.M., 2003. Principles of Animal Locomotion. Princeton University Press, Princeton, NJ, 371 pp.

Arnold, G.P., Greer Walker, M., 1992. Vertical movements of cod (*Gadus morhua* L.) in the open sea and the hydrostatic function of the swimbladder. ICES J. Mar. Sci. 49, 357–372.

Beamish, F.W.H., 1966. Vertical migration by demersal fish in the Northwest Atlantic. J. Fish. Res. Board Can. 23, 109–139.

Blake, R.W., 1979. Energetics of hovering in the mandarin fish (*Synchropus picturatus*). J. Exp. Biol. 82, 25–33.

Brunel, P., 1965. Food as a factor or indicator of vertical migrations of cod in the western gulf of St. Lawrence. ICNAF Spec. Publ. 6, 439–448.

Clark, C.W., Levy, D.A., 1988. Diel vertical migration by juvenile sockeye salmon and the antipredation window. Am. Nat. 131, 271–290.

Clay, C.S., Horne, J.K., 1994. Acoustic models of fish: the Atlantic cod (*Gadus morhua*). J. Acoust. Soc. Am. 96, 1661–1668.

Denton, E.J., Liddicoat, J.D., Taylor, D.W., 1972. The permeability to gases of the swimbladder of the conger eel (*Conger conger*). J. Mar. Biol. Assoc. U.K. 52, 727–746.

Dickson, K.A., Donley, J.M., Sepulveda, C., Bhoopat, L., 2002. Effects of temperature on sustained swimming performance and swimming kinematics of the chub mackerel *Scomber japonicus*. J. Exp. Biol. 205, 969–980.

Drucker, E.G., Lauder, G.V., 1999. Locomotor forces on a swimming fish: three-dimensional vortex wake dynamics quantified using digital particle image velocimetry. J. Exp. Biol. 202, 2393–2412.

Fänge, R., 1953. The mechanisms of gas transport in the euphysoclist swimbladder. Acta. Physiol. Scand. 30 (Suppl. 110), 1–133.

Glasstone, S., Lewis, D., 1964. The Elements of Physical Chemistry. MacMillan & Co, London, 758 pp.

Godø, O.R., Michalsen, K., 2000. Migratory behaviour of north-east Arctic cod, studied by use of data storage tags. Fish. Res. (Amst) 48, 127–140.

Hansson, S., Rudstam, L.G., Kitchell, J.F., Hilden, M., Johnson, B.L., Peppard, P.E., 1996. Predation rates by North Sea cod (*Gadus morhua*)—predictions from models on gastric evacuation and bioenergetics. ICES J. Mar. Sci. 53, 107–114.

Harden Jones, F.R., 1951. The swimbladder and vertical movements of teleost fishes. I. Physical factors. J. Exp. Biol. 28, 553–566.

Harden Jones, F.R., 1952. The swimbladder and vertical movements of teleost fishes. II. The restiction to rapid and slow movements. J. Exp. Biol. 29, 94–109.

Harden Jones, F.R., 1981. Fish migration: strategy and tactics. In: Aidley, D.J. (Ed.), Animal Migration. Cambridge University Press, Cambridge, pp. 139–165.

Harden Jones, F.R., Scholes, P., 1985. Gas secretion and resorption in the swimbladder of the cod *Gadus morhua*. J. Comp. Physiol. B Biochem. Syst. Environ. Physiol. 155, 319–331.

Hewett, S.W., Johnson, B.L., 1992. Fish Bioenergetics Model 2. University of Wisconsin Sea Grant Institute, Madison, 80 pp.

Huse, I., Ona, E., 1996. Tilt angle distribution and swimming speed of overwintering Norwegian spring spawning herring. ICES J. Mar. Sci. 53, 863–873.

Jobling, M., 1995. Environmental biology of fishes. In: Fish and Fisheries Series 16. Chapman & Hall, London, 436 pp.

Kuhn, W., Ramel, A., Huhn, H.J., Marti, E., 1963. The filling mechanism of the swimbladder. Experimentia 19, 497–511.

Lapennas, G.N., Schmidt-Nielsen, K., 1977. Swimbladder permeability to oxygen. J. Exp. Biol. 67, 175–196.

Løkkeborg, S., 1998. Feeding behaviour of cod, *Gadus morhua*: activity rhythm and chemically mediated food search. Anim. Behav. 56, 371–378.

MacLennan, D.N., Simmonds, E.J., 1992. Fisheries Acoustics. Chapman & Hall, London, 325 pp.

Metcalfe, J.D., Arnold, G.P., 1997. Tracking fish with electronic tags. Nature 387, 665–666.

Moyle, P.B., Cech Jr., J.J., 1988. Fishes: an Introduction to Ichtyology. Prentice Hall, Upper Saddle River, New Jersey, 559 pp.

Nakken, O. and Olsen, K. 1977. Target strengths measurements of fish. Rapp. P.-V. Réun. Cons. Int. Explor. Mer, vol. 170, pp. 52–69.

Nauen, J.C., Lauder, G.V., 2002. Hydrodynamics of caudal fin locomotion by chub mackerel, *Scomber japonicus* (Scombridae). J. Exp. Biol. 205, 1709–1724.

Nøttestad, L., 1998. Extensive gas bubble release in Norwegian spring-spawning herring (*Clupea harengus*) during predator avoidance. ICES J. Mar. Sci. 55, 1133–1140.

Ona, E., 1990. Physiological factors causing natural variation in acoustic target strength of fish. J. Mar. Biol. Assoc. U.K. 70, 107–127.

Pelster, B., 2001. The generation of hyperbaric oxygen tensions in fish. News Physiol. Sci. 16, 287–291.

Pelster, B., Scheid, P., 1992. Countercurrent consentration and gas secretion in the swimbladder. Physiol. Zool. 65, 1–16.

Pelster, B., Kobayashi, H., Scheid, P., 1989. Metabolism of the perfused swimbladder of the European eel: oxygen, carbon dioxide, glucose and lactate balance. J. Exp. Biol. 144, 495–506.

Pelster, B., Hicks, J., Driedzic, W.R., 1994. Contribution of the pentose phosphate shunt to the formation of CO_2 in the swimbladder tissue of the eel. J. Exp. Biol. 197, 119–128.

Prosser, C.L. (Ed.), 1973. Comparative Animal Physiology. Saunders, Philadelphia, 966 pp.

Qutob, Z., 1962. The swimbladder of fishes as a pressure receptor. Arch. Neer. Zoo. 15, 1–67.

Reidy, S.P., Kerr, S.R., Nelson, J.A., 2000. Aerobic and anaerobic swimming performance of individual Atlantic cod. J. Exp. Biol. 203, 347–357.

Rose, G.A., Porter, D.R., 1996. Target-strength studies on Atlantic cod (*Gadus morhua*) in Newfoundland waters. ICES J. Mar. Sci. 53, 259–265.

Rosland, R., Giske, J., 1994. A dynamic optimisation model of the diel vertical distribution of a pelagic planktivorous fish. Prog. Ocean. 34, 1–43.

Ross, L.G., 1979. The permeability to oxygen and the guanine content of the swimbladder of a physoclist fish, *Pollchius virens*. J. Mar. Biol. Assoc. U.K. 59, 437–441.

Schmidt-Nielsen, K., 1997. Animal Physiology: Adaptation and Environment. Cambridge University Press, Cambridge, 607 pp.

Scholander, P.F., 1956. Observations on the gas gland in living fish. J. Cell. Comp. Physiol. 48, 523–528.

Scholander, P.F., van Dam, L., 1954. Secretion of gases against high pressure in the swimbladder of deep sea fishes. II. The rete mirabile. Biol. Bull. (Woods Hole) 107, 260–277.

Schurmann, H., Steffensen, J.F., 1997. Effects of temperature, hypoxia and activity on the metabolism of juvenile Atlantic cod. J. Fish Biol. 50, 1166–1180.

Schwerte, T., Axelsson, M., Nilsson, S., Pelster, B., 1997. Effects of vagal stimulation on swimbladder blood flow in the European eel *Anguilla anguilla*. J. Exp. Biol. 200, 3133–3139.

Sepulveda, C., Dickson, K.A., 2000. Maximum sustainable speeds and cost of swimming in juvenile kawakawa tuna (*Euthynnus affinis*) and chub mackerel (*Scomber japonicus*). J. Exp. Biol. 203, 3089–3101.

Steen, J.B., 1963a. The physiology of the swimbladder in the eel *Anguilla vulgaris* III. The mechanism of gas secretion. Acta. Physiol. Scand. 59, 221–241.

Steen, J.B., 1963b. The physiology of the swimbladder in the eel *Anguilla vulgaris* II. The reabsorbtion of gas. Acta. Physiol. Scand. 58, 138–149.

Strand, E., Huse, G., Giske, J., 2002. Artificial evolution of life history and behavior. Am. Nat. 159, 624–644.

Tytler, P., Blaxter, J.H.S., 1973. Adaptation by cod and saithe to pressure changes. Neth. J. Sea Res. 7, 31–45.

Vogel, S., 1994. Life in Moving Fluids: the Physical Biology of Flow. Princeton University Press, Princeton, 467 pp.

Wahlqvist, I., 1985. Physiological evidence for peripheral ganglionic synapses in adrenergic pathways to the swimbladder of the Atlantic cod, *Gadus morhua*. Comp. Biochem. Physiol. 80C, 269–272.

Ware, D.M., 1978. Bioenergetics of pelagic fish: theoretical change in swimming speed and ration with body size. J. Fish. Res. Board Can. 35, 220–228.

Webber, D.M., Boutilier, R.G., Kerr, S.R., 1998. Cardiac output as a predictor of metabolic rate in cod *Gadus morhua*. J. Exp. Biol. 201, 2779–2789.

Weihs, D., 1973. Mechanically efficient swimming techniques for fish with negative buoyancy. J. Mar. Res. 31, 194–209.

Wittenberg, J.B., Copeland, D.E., Haedrich, R.L., Child, J.S., 1980. The swimbladder of deep sea fish: the swimbladder wall is a lipid-rich barrier to oxygen diffusion. J. Mar. Biol. Assoc. U.K. 60, 263–276.